

## Flute Stabilization Due to Ponderomotive Force Created by an rf Field with a Variable Gradient

Y. Yasaka and R. Itatani

*Department of Electronics, Kyoto University, Kyoto 606, Japan*

(Received 19 February 1986)

An rf-stabilization experiment was performed in the axisymmetric single-mirror device HIEI by controlling the radial-gradient scale length of the rf field with the aid of an azimuthally phased antenna array. The flute stability depends sensitively on the scale length of the perpendicular rf electric field, which shows that rf stabilization is caused by the ponderomotive force for ions.

PACS numbers: 52.35.Py, 52.55.Jd

Radio-frequency (rf) stabilization of the flute mode has offered the possibility of operating a tandem mirror in a purely axisymmetric configuration. Experimental demonstration of the stabilization was made in the HIEI<sup>1,2</sup> and Phaedrus<sup>3</sup> devices. The mechanism of stabilization is attributed to the ponderomotive force due to the radial gradient of the rf electric field in both experiments. In HIEI,<sup>4</sup> especially measured was the dependence of the rf field amplitude necessary to stabilize the flute upon plasma density and effective gravity. The result is in quantitative agreement with the theory which includes a nonlocal flute dispersion relation with the radial ponderomotive force.

On the other hand, recent theoretical studies stimulated by the above experiments have proposed two possible mechanisms for rf stabilization, i.e., the ponderomotive effect<sup>5-7</sup> and the sideband-coupling effect.<sup>6-9</sup> Although the models in these theories have many limitations, it appears that both effects depend sensitively on rf frequency and rf amplitude. So, in order to deduce which mechanism is of primary importance in each experiment, it is necessary to measure the correlation between flute stability and rf field structure.

In this Letter, we perform an rf-stabilization experiment using an azimuthally phased antenna array. The radial profile of the excited rf field can be changed by controlling the amplitude and the phase of the rf current in each antenna element. In addition, the plasma is produced by the rf field itself without the use of a plasma gun even in the startup phase. This eliminates line tying between the plasma and the end walls which would affect the flute stability of the plasma. We measure, for the first time, the flute stability when changing the radial profile of the stabilizing rf field. It is shown that the stability changes with the radial-gradient scale length of the rf field strength, in a manner which is in good agreement with the ponderomotive theory.

The HIEI device is an axisymmetric single mirror with mirror length of 1.2 m, maximum magnetic field strength at the throat  $B_M$  of 1.1 T, and mirror ratio

$R = 1.4-4$ , which is variable. The rf antenna located at the midplane consists of four elements aligned axially with  $90^\circ$  intervals in azimuthal direction. Each element, which is a straight bar 33 cm in length and 3 cm in width, is placed at a radial position  $r_A = 4.2$  cm. The wall radius is 7.5 cm. The antenna is driven by two rf amplifiers which can deliver pulsed rf power of up to 250 kW at a frequency  $\omega/2\pi = 8.0$  MHz. Each output of the rf amplifiers is connected to one or two of the four elements through coaxial feeder(s). By adjusting the phase difference between the two rf amplifiers and/or choosing the combination of the feeders and the antenna elements, we can selectively establish rf fields of azimuthal mode  $m = 0, +1, -1, \pm 1$ , or  $\pm 2$ . Here, we assume that the rf field varies as  $\exp[i(m\theta + k_{\parallel}z - \omega t)]$  with  $k_{\parallel}$  being the axial wave number. (It is noted that the  $m = \pm 1$  rf field, for example, consists of  $m = +1$  and  $m = -1$  rf fields of equal amplitude.) Since the amplitude of the perpendicular rf electric field varies as  $AJ_{m-1}(k_{\perp}r) + BJ_{m+1}(k_{\perp}r)$ , with  $A$  and  $B$  being constants determined by plasma parameters, we can control the radial gradient of the electric field through the selection of  $m$ .

The plasma is produced by hydrogen gas puffing from a gas box followed by the application of an rf pulse. The gas box has a slit around the plasma column for azimuthally symmetric gas injection. No startup gun is used, in order to eliminate the line-tying effect. The end-free plasma is sustained for the duration of the rf pulse of up to 10 msec. Since ionization of the gas is mainly caused by the axial electric field  $E_z$  of the antenna near field, the plasma production rate is insensitive to the mode number  $m$  of the rf field. Typical plasma parameters are  $n_0 = (1-2) \times 10^{12}$  cm<sup>-3</sup>,  $T_e = (15-20)$  eV,  $T_i \approx 15$  eV, and  $R = 2.3$  for an power of  $P_{in} \approx 30$  kW. Because  $\omega/\omega_{ci} = 2.3-2.6$ , with  $\omega_{ci}$  being the local ion cyclotron frequency, we have no ion heating by the rf pulse, which is different from other rf-production experiments.<sup>3,10</sup> Thus, we can exclude complications introduced by nonadiabaticity.

As is well known, the radial ponderomotive force

for ions due to linearly polarized rf fields is roughly given by

$$F_p \approx -(e^2/2m_i) E_{\perp}^2 / l_E (\omega^2 - \omega_{ci}^2) \quad (1)$$

for adiabatic conditions. Here,  $m_i$  is the ion mass,  $E_{\perp}$  is the perpendicular rf electric field, and  $l_E$  is the radial scale length of  $E_{\perp}$ . For stabilization of the flute mode, this force must oppose the radial force due to the bad curvature of magnetic field lines. In Phaedrus,<sup>3</sup> it was observed that the fluctuation level due to the flute instability changes sharply from more than 80% to a few percent as  $\omega$  is increased from below  $\omega_{ci}$  to above  $\omega_{ci}$  with other parameters in Eq. (1) approximately fixed. In the previous experiment in HIEI,<sup>2,4</sup> the flute stability was examined as a function of  $E_{\perp}$  with fixed values of  $\omega - \omega_{ci}$  and  $l_E$ . We now compare the flute fluctuations in the cases of rf fields of the same  $\omega - \omega_{ci}$  and  $E_{\perp}$  but different  $l_E$ .

Figure 1 shows an oscillogram of the first 2.5 msec of the plasma density during a shot of 10 msec duration. Let us define  $I_i$  as the value of the current (including phase) of the  $i$ th antenna element ( $i=1-4$ ). The number  $i$  is assigned in a counterclockwise fashion with respect to the static magnetic field. For the rf field corresponding to  $I_1=90$  A,  $I_2=0$ ,  $I_3=90$  A, and  $I_4=0$ , the plasma is very stable with a peak density of  $1.2 \times 10^{12}$  cm<sup>-3</sup> as shown in Fig. 1(a). The gradual decrease in density is due to the decrease of rf power

with time. The other parameters are  $B_M=0.47$  T,  $R=2.3$ , and  $P_{in} \approx 25$  kW. When the values of the rf current are changed so that  $I_1=90$  A,  $I_2=0$ ,  $I_3=-90$  A,  $I_4=0$ , with the other parameters unchanged, the plasma stability changes drastically as shown in Fig. 1(b). The fluctuation level is very large as compared with case (a). Furthermore, the density attained is smaller than in case (a) by a factor of 2. From the correlation measurement, the fluctuation is identified as the flute mode with frequency  $\Omega/2\pi=6-10$  kHz and azimuthal mode  $M=1$ . We observed in case (b) that, for some shots, the plasma density decreased to almost zero even during the rf pulse and recovered again after a few hundred microseconds. The fluctuation level for very low densities was fairly small, but it rapidly increased in the recovering phase.

The radial profile of the rf field is directly measured by a magnetic probe inserted at the midplane. The amplitudes of perpendicular and axial rf magnetic fields,  $B_{\perp}$  and  $B_z$ , are plotted in Figs. 2(a) and 2(b), whose experimental conditions are the same as in Figs. 1(a) and 1(b), respectively. For case (a), the antenna elements drive a combination of  $m = \pm 2$  and  $m = 0$  mode rf fields, while the  $m = \pm 1$  mode rf field is selectively excited for case (b). The perpendicular field is almost linearly polarized inside the plasma for both cases (a) and (b). As is expected, the radial scale length of  $B_{\perp}$ ,  $l_B$ , is controlled by the mode selection. The value of  $l_B$  is  $\sim 4$  cm for case (a) and  $\sim 14$  cm for case (b). The functional dependences of  $B_r$  and  $B_{\theta}$

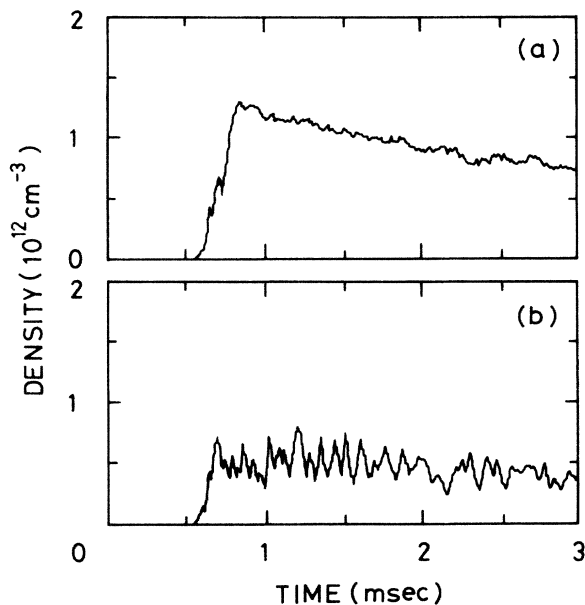


FIG. 1. Oscillograms of the plasma density at  $r=3$  cm for the first 2.5 msec of shots of 10 msec duration. Only the combination of the antenna currents is changed between the two shots. (a)  $I_1=90$  A,  $I_2=0$ ,  $I_3=90$  A, and  $I_4=0$ ; (b)  $I_1=90$  A,  $I_2=0$ ,  $I_3=-90$  A, and  $I_4=0$ . The mode of the rf field is  $m = \pm 2$  and 0 for (a) and  $m = \pm 1$  for (b).

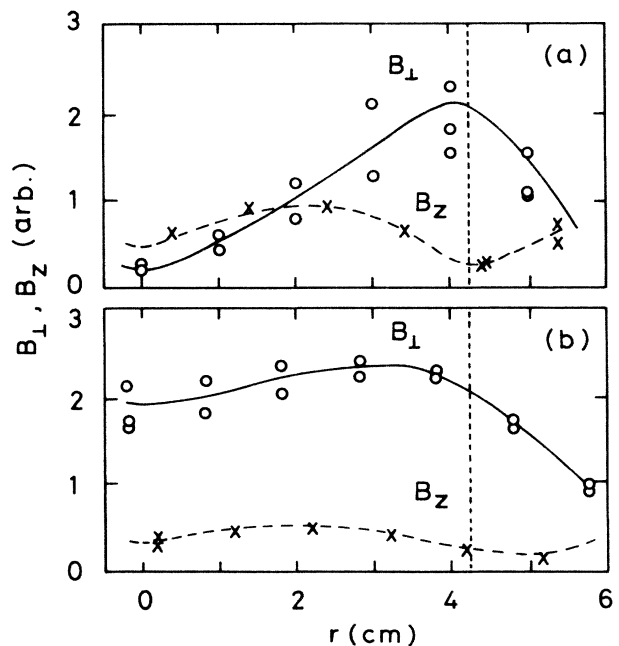


FIG. 2. Radial distribution of perpendicular and axial rf magnetic fields at the midplane. Cases (a) and (b) correspond to those in Fig. 1.

on  $r$  are respectively the same as those of  $E_\theta$  and  $E_r$ , provided that  $E_z$  is small. (This is confirmed by a calculation using Hojo and Hatori's RF code.<sup>11</sup>) Hence, we can use the value of  $l_B$  as the radial scale length of  $E_\perp$  ( $l_E \approx l_B$ ). Theoretically,  $B_z$  has a functional form of a combination of  $J_2(k_\perp r)$  and  $J_0(k_\perp r)$  for case (a), and of  $J_1(k_\perp r)$  for case (b). The measured  $B_z$  profiles are consistent with the predictions. According to Eq. (1), we note that the radial ponderomotive force is radially inward and, thus, stabilizing for both cases (a) and (b), but the magnitude of the ponderomotive force for case (a) is about 3.5 times larger than for case (b). It is estimated that the centrifugal force due to the bad field-line curvature,  $F_c$ , is  $5.6 \times 10^{-19}$  N. Since  $E_\perp$  is calculated from the measured  $B_\perp$  to be 22 V/cm at  $r \approx 3$  cm, the ratio of  $F_p$  to  $F_c$  is roughly 3 for case (a) and 0.9 for case (b). The dramatic change in stability observed in Fig. 1 is attributed to the change in the radial ponderomotive force caused by the difference in  $l_E$ .

The four antenna elements were then excited simultaneously. For  $I_1 = I_2 = -I_3 = -I_4$ , the excited rf field is of  $m = \pm 1$  mode, while the combination  $I_1 = -I_2 = I_3 = -I_4$  provides  $m = \pm 2$ . So, by a change of the relative phase and amplitude of  $I_2$  and  $I_3$  with respect to  $I_1$  and  $I_4$ , the excited rf mode can be varied from pure  $m = \pm 1$  to pure  $m = \pm 2$  through a mixture of  $m = \pm 1$  and  $\pm 2$ . This change in mode number results in a change in  $l_B$ . Controlling the value of  $l_B$  in this way, we measured the flute stability. The result is shown in Fig. 3, where the density fluctuation level is plotted as a function of  $B_\perp^2/l_B$ . The factor  $B_\perp^2$  is included in order to compensate for a vari-

ation in  $B_\perp$ , which is less than 15%, when changing  $l_B$ . As the variation is small, the change in abscissa is predominantly caused by  $l_B$ . For smaller values of  $B_\perp^2/l_B$ , the  $m = \pm 1$  mode component is larger than the  $m = \pm 2$  mode component, and vice versa. We see that the fluctuation level is smoothly decreasing with shorter  $l_B$ . In the previous experiment,<sup>2,4</sup> it was observed that the fluctuation level of the flute mode decreased when  $B_\perp$  was increased. It is evident from Fig. 3 that the fluctuation level is also dependent on the radial-gradient scale length of the rf field. The flute stabilization with a fluctuation level of less than 20% is obtained when  $l_B (\approx l_E) < 5.6$  cm, which corresponds to  $F_p/F_c > 2.1$ . Although we need a nonlocal theory of the flute stability including pressure-weighted bad-curvature effects in order to explain the result in Fig. 3 quantitatively, the overall dependence of the stability on  $l_E$  as well as  $E_\perp$  is in good agreement with Eq. (1), showing that the observed rf stabilization is due to the ponderomotive force for ions created by the perpendicular rf electric field.

The ponderomotive effect on electrons is negligible as discussed in the following. Since  $E_\perp$  is estimated to be almost linearly polarized from the measured polarization of  $B_\perp$ , there arises little ponderomotive force for electrons due to  $E_\perp$ . The ponderomotive force due to the radial gradient of  $E_z$  could become larger than  $F_p$  because of the large mass ratio. If so, the magnitude and/or the radial scale length of  $E_z$  must change significantly between the two shots in Fig. 1 to produce the change in the stability. We measured the radial profile of  $T_e$ , which is considered to reflect that of  $E_z$ , for the two cases to find that the profile is almost flat ( $T_e = 17 \pm 3$  eV) for all plasma radii and changes by no more than 3 eV between the two cases. This is indirect confirmation that the profile and the magnitude of  $E_z$  remain unchanged when the plasma goes from stable to unstable. The calculation of  $E_\perp$  and  $E_z$  by Hojo and Hatori's RF code shows that  $E_z$  is an order of magnitude smaller than  $E_\perp$  and has a much larger scale length than  $E_\perp$ . Furthermore, the ratio of collision frequency for electrons to  $\omega$  is 0.1–0.5. These facts show that the ponderomotive force for electrons cannot contribute to the flute stabilization for the present experimental conditions.

Another possible stabilization mechanism is the sideband-coupling effect. McBride, Stefan, and Krall<sup>9</sup> calculated the mode coupling between the flute mode and the electrostatic sideband modes created by the beating of the flute mode and the applied linearly polarized rf with arbitrary wave number, using the local approximation. They showed that, for small  $k_\parallel/k_r$ , with  $k_r$  being the radial component of the wave number of the applied rf, the flute mode is stabilized only when  $\omega < \omega_{ci}$ . In the experiment, however, the flute stabilization is observed for  $m = \pm 2$  rf field

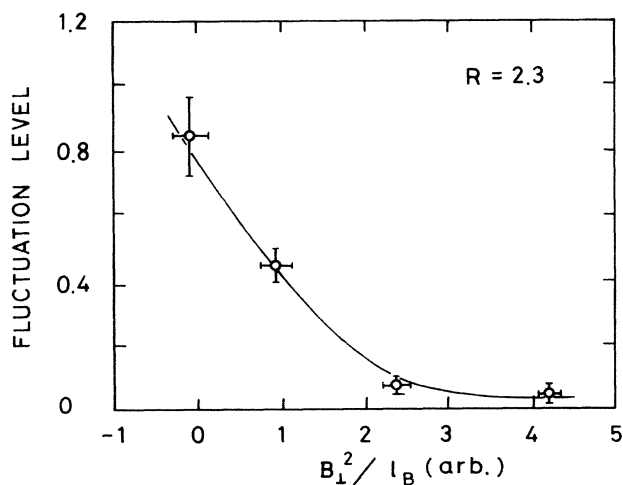


FIG. 3. Fluctuation level of flute instabilities vs  $B_\perp^2/l_B$  for  $\omega/\omega_{ci} = 2.3$  and  $R = 2.3$ . The rf field is a mixture of  $m = \pm 1$  mode and  $m = \pm 2$  mode. For larger values of  $B_\perp^2/l_B$ , the  $m = \pm 2$  component is larger than  $m = \pm 1$ .

when  $\omega > \omega_{ci}$ . This result is inexplicable by the theory.

In the paper by Cohen and Rognlien,<sup>6</sup> the flute stability is calculated including the ponderomotive and the sideband-coupling effects separately for left-hand circularly polarized rf field with  $k_{\parallel} = 0$ . It is shown that when

$$A \equiv (M/r_0) l_N \gamma_g \omega / 2(\omega - \omega_{ci})^2 \gg 1,$$

the sideband-coupling stabilization dominates the ponderomotive stabilization and vice versa, where  $\gamma_g$  is the local growth rate of the flute mode,  $l_N$  is the radial-density scale length, and  $r_0$  is the radius where the flute mode has a maximum amplitude. In the present experiment with  $M=1$ ,  $r_0 \approx 3$  cm,  $\gamma_g/\omega_{ci} \approx 6 \times 10^{-3}$ , and  $\omega/\omega_{ci} = 2.3$ , the value of  $A$  is  $\sim 10^{-2}$ . So, according to their theory the stabilization should come from the ponderomotive effect. But the theory assumes  $m=0$  and  $k_{\parallel} = 0$ , which are not satisfied in our experiment.

Recently, D'Ippolito and Myra<sup>7</sup> presented a unified theory of the ponderomotive and electromagnetic-sideband-mode-coupling effects with finite  $k_{\parallel}$  and  $m$  of order unity. Although the local approximation is still necessary to obtain an analytic result, the theory is most relevant to the present experiment. The growth rate of the flute mode is given by  $\gamma^2 = \gamma_g^2 - \gamma_p^2 - \gamma_s^2$ , where  $\gamma_p$  and  $\gamma_s$  are respectively ponderomotive and sideband-coupling terms. It is shown that  $\gamma_s^2$  is proportional to the sideband field amplitude which is proportional to  $E_{\perp}/D$ , where  $D$  is the determinant of the coefficient matrix of the wave equation and, hence,  $D=0$  gives the dispersion relation of the sideband wave. This shows that  $\gamma_s^2$  can become large if the sideband wave satisfies the dispersion relation. For the case of  $m = \pm 1$  and  $m = \pm 2$  rf application in the experiment, the azimuthal modes of the sideband are predicted to be  $m_s \equiv M \pm m = 0, 2, 1$ , and  $3$ . Since the  $m_s = 0$  mode is cut off in the present range of  $\omega$ , the possible sidebands are  $m_s = 1, 2$ , and  $3$  fast waves which are right-hand circularly polarized for almost all plasma radii. By using Eqs. (38), (39), and (41) in Ref. 7,  $\gamma_s^2$  is calculated to be

$$\sim G(1/l_N^2)(1 + \alpha^2)E_{\perp}^2 R(R - L)/2(R + L - 2n_{\parallel}^2),$$

where  $G = \epsilon_0/4n_0m_i$ ,  $R = \omega_{pi}^2/\omega_{ci}(\omega + \omega_{ci})$ ,  $L = -\omega_{pi}^2/\omega_{ci}(\omega - \omega_{ci})$ ,  $n_{\parallel} = k_{\parallel}c/\omega$ ,  $\epsilon_0$  is the permittivity in vacuum, and  $\alpha$  is the fraction of  $m = \pm 2$  spectral component in the rf field composed of a mixture of  $m = \pm 1$  and  $m = \pm 2$  modes. We have used

$m/r_0 \gg k_{\parallel}$  and  $\omega_s \equiv \omega \pm \Omega \approx \omega$ . As  $R$  is positive,  $L$  is negative, and  $|L| > R$ , we see that  $\gamma_s^2 < 0$ , resulting in a destabilizing effect. On the other hand, the ponderomotive term is given by  $\sim G(1/l_N l_E)E_{\perp}^2(R + L)$ , which is equal to  $l_N f_p/m_i$ . For  $l_E > 0$ , this term is stabilizing. At a point where  $B_{\perp}^2/l_B = 1.6$  in Fig. 3 ( $l_E \approx 6$  cm and  $\alpha \approx 0.6$ ), the ratio of  $|\gamma_s^2|$  to  $|\gamma_p^2|$  ranges from 0.4 to 0.08, corresponding to  $0 \leq k_{\parallel} \leq 10$  m<sup>-1</sup>. This ratio becomes smaller for larger  $B_{\perp}^2/l_B$ . Hence the theory predicts that, for any  $k_{\parallel}$  which the antenna can generate, ponderomotive stabilization will dominate destabilization by sideband coupling when  $l_E < 6$  cm. The contribution from  $E_z$  in the sideband-coupling term is negligible because of collisional effects as discussed before. Thus, the flute stabilization observed for  $l_E < 6$  cm cannot be attributed to sideband coupling. This is because  $\omega$  is far from  $\omega_{ci}$  and  $\gamma_g^2$  is small.

In summary, we have performed an rf stabilization experiment by controlling the radial-gradient scale length of the rf field with the aid of an azimuthally phased antenna array. The flute stability depends sensitively on the scale length of the perpendicular rf electric field, showing that the rf stabilization is caused, in this experiment, by the ponderomotive force for ions. Thus, the end-free, stable plasma can be started up and sustained solely by rf with no MHD anchor.

The authors would like to acknowledge assistance by H. Takeno and F. Kobayashi. This work was supported by a Grant in Aid for Scientific Research from the Japanese Ministry of Education.

<sup>1</sup>M. Inutake *et al.*, in *Proceedings of the Ninth International Conference on Plasma Physics and Controlled Nuclear Fusion Research, Baltimore, 1982* (International Atomic Energy Agency, Vienna, 1983), Vol. 1, p. 545.

<sup>2</sup>Y. Yasaka and R. Itatani, *Nucl. Fusion* **24**, 445 (1984).

<sup>3</sup>J. Ferron *et al.*, *Phys. Rev. Lett.* **51**, 1955 (1983).

<sup>4</sup>Y. Yasaka and R. Itatani, *Nucl. Fusion* **25**, 29 (1985).

<sup>5</sup>J. Myra and D. D'Ippolito, *Phys. Rev. Lett.* **53**, 914 (1984).

<sup>6</sup>B. Cohen and T. Rognlien, *Phys. Fluids* **28**, 2194 (1985).

<sup>7</sup>D. D'Ippolito and J. Myra, Science Applications Report No. SAIC-85/1922 PRI-94, 1986 (to be published).

<sup>8</sup>J. McBride, *Phys. Fluids* **27**, 324 (1984).

<sup>9</sup>J. McBride, V. Stefan, and N. Krall, *Phys. Rev. Lett.* **54**, 42 (1985).

<sup>10</sup>R. Kumazawa *et al.*, in Ref. 1, p. 565.

<sup>11</sup>H. Hojo and T. Hatori, private communication.